Metal−Metal Bonding and Structures of Metal String Complexes $Cr_3(dpa)_4Cl_2$, $Cr_3(dpa)_4(NCS)_2$, and $[Cr_3(dpa)_4Cl_2](PF_6)$ from IR, Raman, and Surface-Enhanced Raman Spectra

Chung-Jen Hsiao,[†] Szu-Hsueh Lai,[†] I-Chia Chen,*[,†] Wen-Zhen Wang,[‡] and Shie-Ming Peng[‡]

Department of Chemistry, National Tsing Hua University, 101 Kuang Fu Road Section 2, Hsinchu, Taiwan 30013, Republic of China, and Department of Chemistry, National Taiwan University, Taipei, Taiwan 10617, Republic of China

Received: September 12, 2008; Revised Manuscript Received: October 17, 2008

We recorded infrared, Raman, and surface-enhanced Raman scattering (SERS) spectra of metal−string complexes $Cr_3(dpa)_4X_2$ (dpa = di(2-pyridyl)amido, X = Cl, NCS) and $[Cr_3(dpa)_4Cl_2](PF_6)$ and dipyridylamine (Hdpa) to determine their vibrational frequencies and to study their structures. For the SERS measurements these complexes were adsorbed on silver nanoparticles in aqueous solution to eliminate the constraints of a crystal lattice. From the results of analysis of the vibrational normal modes we assign the infrared band at 346 cm^{-1} to the Cr_3 asymmetric stretching vibration of the symmetric form and the Raman line at 570 cm^{-1} to the Cr−Cr stretching mode for the unsymmetric form of $Cr_3(dpa)_4Cl_2$. Complex $Cr_3(dpa)_4Cl_2$ exhibits both symmetric (*s*-) and unsymmetric (*u*-) forms in solution but $Cr_3(dpa)_4(NCS)_2$ only the *s*-form. The structures for both complexes in their ground states have the *s*-form. The oxidized complex $[Cr_3(dpa)_4Cl_2](PF_6)$ has only a *u*-form for which the Cr−Cr stretching mode is assigned to the band at 570 cm^{-1}. From the variation with temperature from 23 to 60 °C of the intensity of this line, we obtained the proportion of the *u*-form $Cr_3(dpa)_4Cl_2$; the enthalpy change is thus obtained to be $\Delta H = 46.2 \pm 3.3$ kJ mol^{-1} and the entropy change is $\Delta S = 138 \pm 10.3$ J K^{-1} mol^{-1} for the reaction *u*-$Cr_3(dpa)_4Cl_2 \leftrightarrow$ *s*-$Cr_3(dpa)_4Cl_2$. From the spectral intensities and band frequencies in SERS spectra, Hdpa is expected to adsorb on a silver nanoparticle with the amido nitrogen and pyridyl rings tilted from the silver surface, whereas the trichromium complex with the chromium ion line is orthogonal to the silver surface normal in aqueous silver solution.

Introduction

Trimetal complexes $M_3(dpa)_4X_2$ (M = Cu,[1,2] Ni,[3−8] Co,[9−20] Cr,[21−26] etc., dpa = di(2-pyridyl)amido) are the simplest metal string complexes with polypyridylamine ligands coordinated helically to linear metal ions. These complexes with unique electric and magnetic properties have prospective applications as nanoscale molecular wires. Among those complexes tricobalt and trichromium complexes have attracted the most attention because according to their X-ray crystal structures they exhibit structures with both symmetric and unsymmetric metal−metal bonding. For unsymmetric (*u*-) $Co_3(dpa)_4Cl_2$ with unequal Co−Co bond distances, Clérac et al. showed that the infrared spectra of this complex displays split pyridyl lines.[14] Lai et al. reported both IR and Raman spectra of complexes $Co_3(dpa)_4Cl_2$ and $Ni_3(dpa)_4Cl_2$ in solid form; they showed split Raman lines of the in-plane deformation of the pyridyl ring for *u*-$Co_3(dpa)_4Cl_2$ and a single line for $Ni_3(dpa)_4Cl_2$ that exists only as a symmetric structure;[27] they also assigned the vibrational frequencies of the Ni_3 stretching and Co_3 asymmetric stretching modes of these complexes that agree with a trend predicted with simple molecular-orbital theory.

From the crystal structure of $Cr_3(dpa)_4Cl_2$, Cotton et al. determined that the complex has a symmetric Cr−Cr bond of length 2.36 Å;[21] after study of other trichromium complexes they suggested that complex $Cr_3(dpa)_4XY$ would have an *u*-form with unequal Cr−Cr bond distances when X ≠ Y,[26] for the X = Y the *s*-form exists only for ligands that act as strong σ donor, for example X = CN, CCPh, etc. Hence, for $Cr_3(dpa)_4Cl_2$ in which Cl is a weak σ donor ligand, unsymmetric structure is expected. Using density-functional theory, Rohmer and Benard found that, without a constraint of a crystal lattice, $Cr_3(dpa)_4Cl_2$ exists in a symmetric form in the ground state.[28,29] Measurements of the effective magnetic moment for a trichromium complex indicate spin $S = 2$ that remains constant for temperatures to 350 K.[23] Rohmer and Bénard proposed an unsymmetric structure to exist also as a quintet state but at greater energy.[29]

The bond order predicted from simple extended Huckel theory for symmetric trichromium ions Cr_3^{6+} is 1.5 and for the *u*-form it is the quadruple bonding for the bonding pair and no bonding for the other pair. In terms of electric conductance they may present different properties because of distinct bonding character. Compared with the other trimetal complexes Ni_3 and Co_3, the *s*-form of Cr_3 has the best electric conductance.[30] The motivation of our work is to identify structures of *s*- and *u*-forms of $Cr_3(dpa)_4Cl_2$ and $Cr_3(dpa)_4(NCS)_2$, using vibrational spectroscopy. These complexes have axial ligand Cl and NCS with weak and strong σ donating ability, respectively. In addition the metal−metal bonding strength is undetermined experimentally for trichromium metal string complexes. The oxidized form $[Cr_3(dpa)_4Cl_2]PF_6$ that has been shown to exist as the *u*-form exclusively is also studied for comparison. We employed surface-enhanced Raman scattering (SERS) spectroscopy to record the vibrational spectra for molecules in solution phase to remove the crystal lattice constraint. Presumably this provides

* To whom correspondence should be addressed. E-mail: icchen@mx.nthu.edu.tw.
[†] National Tsing Hua University.
[‡] National Taiwan University.

10.1021/jp8081326 CCC: $40.75
Published on Web 11/24/2008

SCHEME 1: Chemical Structures of (a) Symmetric and (b) Unsymmetric $Cr_3(dpa)_4Cl_2$, (c) $Cr_3(dpa)_4(NCS)_2$, and (d) $[Cr_3(dpa)_4Cl_2](PF_6)$ and Their Bond Lengths (Å) taken from References 28 and 31, Respectively

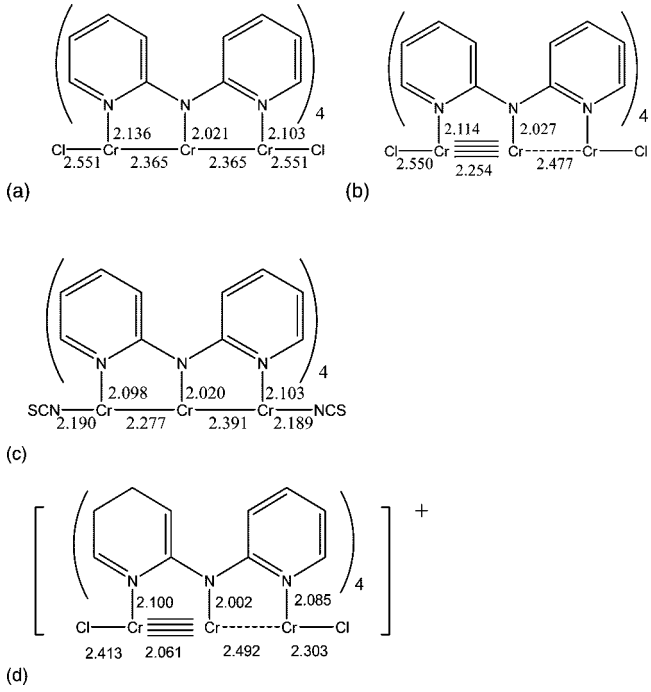

the information of molecular structure under thermal equilibrium. Vibrational spectra of dipyridylamine, Hdpa, are also investigated to assist in the vibrational normal-mode analysis for metal string complexes. The structures of $Cr_3(dpa)_4Cl_2$, $Cr_3(dpa)_4(NCS)_2$, and the oxidized form $[Cr_3(dpa)_4Cl_2]^+$ for reference, from X-ray crystal data,[26,31] are displayed in Scheme 1.

Experimental Section

The solid metal complexes and dipyridylamine, Hdpa, were synthesized according to methods described elsewhere.[5,9,22,32] Compound $Cr_3(dpa)_4X_2$ was purified by recrystallization from a solution of CH_2Cl_2 at room temperature. IR absorption spectra in the far-infrared region 150−650 cm^{-1} were recorded at the NTHU Instrument Center (Bomem FTIR spectrometer). A solid sample was mixed with CsI at a ratio 1:1−2 for the low-wavenumber range to obtain sufficient absorbance. The Raman spectra were recorded in a backscattering geometry to improve the ratio of signal-to-noise; the spectral resolution, 3 cm^{-1}, was limited by the monochromator (length 0.6 m, grating with 600 grooves/mm). A He−Ne laser (wavelength 632.8 nm) served as the excitation source; the laser power at the sample was set at 15 mW. The scattered signal passing through a notch filter was recorded with a thermoelectrically cooled CCD detector. Samples for SERS measurements were prepared on adding complexes to an aqueous solution of silver nanoparticles (diameter 65−75 nm). The silver nanoparticles were prepared by reduction of silver nitrate with sodium citrate. The greenish-yellow particles display plasmon absorption with a maximum at 420 nm. The integration period was typically about 30 s for a solid sample and 1 s for SERS, and was averaged for 100 scans. All spectra were recorded under room temperature except as indicated. To avoid self-absorption for Raman measurements on solid samples, the complex was mixed with KBr at a ratio of 1:10.

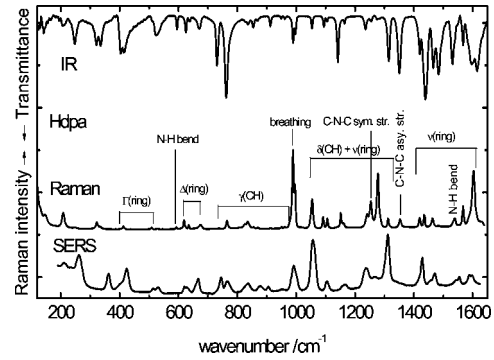

Figure 1. IR and Raman spectra (150−1650 cm^{-1}) of Hdpa in a solid form and the SERS spectrum of Hdpa on silver nanoparticles in aqueous solution, recorded at excitation wavelength 632.8 nm. ν denotes a stretching mode, γ and δ in-plane bending and out-of-plane bending, and Δ and Γ pyridyl ring in-plane and out-of-plane twisting modes, respectively.

Quantum-chemical calculations based on density-functional theory (DFT) were performed to obtain optimized geometries, vibrational wavenumbers, and both Raman and IR intensities; the B3LYP method with basis set 6-31G* was employed for Hdpa to achieve reliable results. All calculations were performed with the GAUSSIAN 03 program.[33]

Results and Discussion

Spectra and Analysis for Hdpa. Hdpa, $C_{10}H_9N_3$ with molecular symmetry group C_2, has 60 vibrational normal modes; all are both IR and Raman active. Among those each pyridyl has 24 vibrational normal modes, and two pyridyls account for 48 modes. The other 12 vibrational modes are comprised of six for motions of C−N(H)−C, N−H out-of-plane bending, N−H in-plane bending, N−H stretching, C−N−C bending, symmetric, and asymmetric stretching and six for motions between pyridyl rings, one ring−ring stretching, two in-plane deformation, and three out-of-plane deformation. Figure 1 displays the IR, Raman, and SERS spectra of Hdpa in the wavenumber range 150−1650 cm^{-1}. The line positions in the IR and Raman spectra agree within 2−3 cm^{-1}; small deviations result from measurement uncertainties.

Full analyses of vibrational normal modes were made based on comparison of the observed spectra, results calculated by using the DFT method and the reported vibrational frequencies of pyridine. Table 1 lists the observed and the calculated line positions and assignments of vibrational motions. In general the vibrational frequencies of the pyridyl moiety agree with the calculated positions, but because the calculated results were based on an isolated structure whereas Hdpa in a solid form and has hydrogen bonding between two molecules, we expect some line splitting and frequency shifts; for example, lines at 989 and 995 cm^{-1} are observed whereas the calculated results show a single line at 975 cm^{-1}. The assignments for modes other than those of pyridyl are as follows: a line at 593 cm^{-1} is assigned to the N−H out-of-plane bending, 1540 cm^{-1} to N−H in-plane bending, 1254 and 1353 cm^{-1} to C−N−C symmetric and asymmetric stretching, respectively, and 247 cm^{-1} to C−N−C bending. Vibrational modes for pyridyl−pyridyl ring−ring motion are expected to lie at low frequencies; a line at 207 cm^{-1} is assigned to ring−ring wagging, 142 cm^{-1} to scissoring, 321 cm^{-1} to stretching, and 335 cm^{-1} to rocking. The remaining two out-of-plane ring−ring motions have low frequencies beyond our detection limit.

The SERS spectrum recorded in aqueous solution differs from the Raman spectrum of a solid sample in spectral intensity, line

TABLE 1: Infrared, Raman, SERS, and Calculated Line Positions (cm^{-1}), Relative Intensity, and Assignments for Hdpa

experimental					calculated		
IR		Raman		SERS	B3LYP/6-31G*		
ν	I	ν	I	ν	$\nu \times 0.97$	symmetry	assignment and mode description[a]
					41	B	butterfly, Γ(ring−ring)
					50	A	ring−ring twisting, Γ(ring−ring)
142	m	147	m		111	A	ring−ring scissoring, Γ(ring−ring)
207	w	208	m	211	205	A	ring−ring wagging, Γ(ring−ring)
247	m	248	vw	262	215	B	C−N−C bending
321	m	323	m	363	314	A	ring−ring stretching, ν(ring−ring)
335	m	332	w		316	B	ring−ring rocking, Γ(ring−ring)
403	m	403	vw	408	406	B	pyridyl 16a, Γ(ring)
413	m	414	w	424	413	A	pyridyl 16a, Γ(ring)
509	vw	509	w	514	498	B	pyridyl 16b, Γ(ring)
525	m	527	vw	530	505	A	pyridyl 16b, Γ(ring)
595	m	593	w		579	B	N−H out-of-plane bending
		619	m	620	603	A	pyridyl 6a, Δ(ring)
625	w				612	B	pyridyl 6a, Δ(ring)
639	vw	635	w	629	617	B	pyridyl 6b, Δ(ring)
670	w	675	w	668	665	A	pyridyl 6b, Δ(ring)
731	s				723	B	pyridyl 4, γ(CH)
		737	vw	744	738	A	pyridyl 4, γ(CH)
762	vs				758	B	pyridyl 11, γ(CH)
		765	m	766	761	A	pyridyl 11, γ(CH)
836	vw	836	m	837	808	A	pyridyl 1, breathing
854	w	855	vw	877	843	B	pyridyl 10a, γ(CH)
869	vw	869	vw		864	A	pyridyl 10a, γ(CH)
912	w	912	vw	905	905	B	pyridyl 1, breathing
949	vw	951	vw		949	B	pyridyl 17a, γ(CH)
961	vw	961	vw		950	A	pyridyl 17a, γ(CH)
					969	B	pyridyl 5, γ(CH)
990	m	989	vs	991			pyridyl 5, γ(CH)
997	w	995	s		975	A	pyridyl 5, γ(CH)
					1034	B	pyridyl 18a, δ(CH) + ν(ring)
1054	w	1054	s	1057	1039	A	pyridyl 18a, δ(CH) + ν(ring)
1094	w	1092	m		1078	B	pyridyl 18b, $\ddot{\delta}$(CH) + ν(ring)
1105	vw	1106	m	1104	1093	A	pyridyl 18b, δ(CH) + ν(ring)
1142	s	1151	m		1139	B	pyridyl 15, δ(CH) + ν(ring)
1164	vw	1163	w	1166	1149	A	pyridyl 15, δ(CH) + ν(ring)
1236	w	1241	m	1237	1210	B	pyridyl 14, δ(CH) + ν(ring)
1255	vw	1254	s	1266	1242	A	C−N−C symmetric stretching
1275	vw	1278	vs		1273	B	pyridyl 3, δ(CH) + ν(ring)
1285	vw				1274	A	pyridyl 14, δ(CH) + ν(ring)
1315	s	1312	m	1311	1307	A	pyridyl 3, δ(CH) + ν(ring)
1351	s	1353	m		1316	B	C−N−C asymmetric stretching
1420	m	1420	m	1429	1407	B	pyridyl 19b, ν(ring)
1439	vs	1435	m		1425	B	pyridyl 19b, ν(ring)
1466	s	1463	m	1470	1433	A	pyridyl 19a, ν(ring)
1484	s	1484	vw		1457	A	pyridyl 19a, ν(ring)
1532	s	1540	m		1512	B	N−H in-plane bending
		1567	s	1545,1555	1563	A	pyridyl 8a, ν(ring)
1568	m				1566	B	pyridyl 8a, ν(ring)
1596	s			1588	1576	B	pyridyl 8b, ν(ring)
1615	s	1602	vs	1597	1592	A	pyridyl 8b, ν(ring)

[a] Wilson notation for vibrational modes of pyridyl is used. Symbols are defined in Figure 1.

width, and line positions for some vibrations. The SERS spectral lines are broad with a full width at 15−20 cm^{-1} at half-maximum (fwhm) whereas it is at 6−8 cm^{-1} for the solid sample. The lines of N−H in-plane and out-of-plane bending disappear in SERS indicating that Hdpa became deprotonated and adsorbed onto the silver nanoparticle with the amido nitrogen in this weakly basic solution. For lines at large wavenumbers, the shifts are typically less than 5 cm^{-1} from the corresponding Raman lines except that lines at 1602 and 1567 cm^{-1} are shifted and split to 1597, 1588 cm^{-1} and 1555, 1545 cm^{-1}, respectively. A line at low wavenumber appearing in the normal Raman spectrum at 248 cm^{-1} that is assigned to C−N−C bending is shifted to 262 cm^{-1}, indicating a stiffer C−N−C bonding after deprotonation. Lines at 323 and 414 cm^{-1} that are assigned as pyridyl−pyridyl ring−ring and pyridyl ring motions, respectively, are also shifted to 363 and 424 cm^{-1}. This condition implies rigid pyridyl rings when bonded to a silver nanoparticle.

The line assigned to the ring breathing mode is split for the solid sample but became broader in silver solution with no shift; similar results were observed for the other pyridyl modes implying no direct π interaction of pyridyl with the silver surface.[34,35] The spectral intensities of lines, for example, at 363, 424, 668, 1057, 1311, and 1429 cm^{-1} assigned to vibrational modes with *a* symmetry, are relatively enhanced. According to the surface selection rules for Raman intensity,[36] modes with

TABLE 2: Infrared and SERS Line Positions (cm^{-1}) and Assignments for $Cr_3(dpa)_4Cl_2$, $Cr_3(dpa)_4(NCS)_2$, and $[Cr_3(dpa)_4Cl_2]^+(PF_6)^-$

$Cr_3(dpa)_4(NCS)_2$		$Cr_3(dpa)_4Cl_2$		$[Cr_3(dpa)_4Cl_2]^+PF_6^-$		
SERS	IR	SERS	IR	SERS	IR	assignment and mode description[a]
147			154	157		Γ(ring−ring)
163			173			Cr−N bending
			184		200	Cr−Cl stretching
211		213		212	211	Γ(ring−ring) + Cr−N bending
249		251	250	251	241	Cr−N stretching
265		265		265		C−N−C bending + Cr−N stretching
	275		275			Cr−Cr−Cr bending
300	304	303	305	303	298, 303	Cr−N stretching
334	330		326		328	Cr−N stretching
	347		346			Cr−Cr−Cr asymmetric stretching
365	361	365	362	364	363	Δ(ring−ring)
398	386	400	388	400	397	Cr−N stretching
429	422	429	419	424	425	pyridyl 16a
446	435	446	435	445	438	pyridyl 16a
489	490					SCN bending
516	519		517		518	pyridyl 16b
536	539		538		539	pyridyl 16b
		570		570		Cr−Cr stretching
628		629	623	629		pyridyl 6a
648	647	649	646	666	654	pyridyl 6b
693		692	675	691		pyridyl 6b
723	740,750		737,749		742, 751	pyridyl 4
	764		766		770	pyridyl 11
	799					C−S stretching
	860		861		863	pyridyl 10a
	882		879		881	pyridyl 10a
924	918	924	919	924	917	pyridyl 1
953	962		974		968	pyridyl 17a
996	979		989		990	pyridyl 17a
1019	1018	1020	1017	1019	1021	pyridyl 5 + pyridyl 12
1058	1055	1058	1055	1058	1057	pyridyl 18a
1114	1112	1116	1111	1114	1113	pyridyl 18b
1157	1158	1162	1154,1167	1157	1158	pyridyl 15
	1244		1243		1246	pyridyl 14
1255	1268	1254	1269	1256		C−N−C symmetric stretching
1272		1273		1272		pyridyl 3
	1281		1284		1284	pyridyl 14
1311	1313	1311	1313	1311	1313	pyridyl 3
1372	1370	1371	1363	1372	1367	C−N−C asymmetric stretching
1429	1428	1429	1431	1429	1428	pyridyl 19b
1445		1445		1445		pyridyl 19b
1465	1465	1466	1468	1465	1466	pyridyl 19a
1478		1480		1478		pyridyl 19a
1559	1549	1559	1548	1559	1550	pyridyl 8a
1598	1597	1599	1596	1598	1598	pyridyl 8b
1611	1608	1614	1607	1611	1608	pyridyl 8b

[a] Wilson notation for vibrational modes of pyridyl is used. Symbols are defined in Figure 1.

vibrational motion vertical to the surface are intense but those with parallel motion are weak. When the molecule lies vertical to the silver surface, the molecular C_2 axis is orthogonal to the surface; modes with vertical vibrational motion belong to the *a* symmetry class. Furthermore, lines for C−N−C symmetric and antisymmetric stretching modes are not observed in SERS because these motions are parallel to the surface. According to the spectral intensity and band positions, the molecule is thus expected to lie vertically with a tilted angle from the surface. Bands with broad features might result from pyridyl rings twisted at various angles to the amido moiety in solution, being released from constraints of the crystal lattice.

Spectra and Analysis for Cr_3 Complexes. Each trichromium complex has four dpa ligands of which the vibrational lines overlap under the experimental conditions, and thus become undifferentiated, but because these metal complexes have high symmetry their IR and Raman spectra are to some extent complementary. Complexes *u*-$Cr_3(dpa)_4Cl_2$ and $Cr_3(dpa)_4(NCS)_2$ belong to symmetry group C_4 in solid form because the axial ligand NCS of the latter complex is tilted from the Cr_3^{+6} ion line whereas *s*-$Cr_3(dpa)_4Cl_2$ has symmetry group D_4. In C_4 all symmetry species are both Raman and IR active except that modes with *b* symmetry are only Raman active. In D_4 vibrational modes with symmetry b_1 and b_2 appear only in Raman, and a_2 in IR. Figures 2−5 display the IR and SERS spectra of $Cr_3(dpa)_4Cl_2$, $Cr_3(dpa)_4(NCS)_2$, and $[Cr_3(dpa)_4Cl_2](PF_6)$, respectively. As the complexes in a solid form decomposed under laser radiation over a protracted period, Raman spectra were unattainable. Table 2 lists the observed line positions and mode assignments. The SERS and IR spectra of Cr complexes exhibit features generally similar to those of Hdpa in the range 410−1600 cm^{-1}, in which most pyridyl vibrations are located. The SERS lines are narrower than those of Hdpa indicating that the twisting angle of pyridyl rings is essentially fixed upon

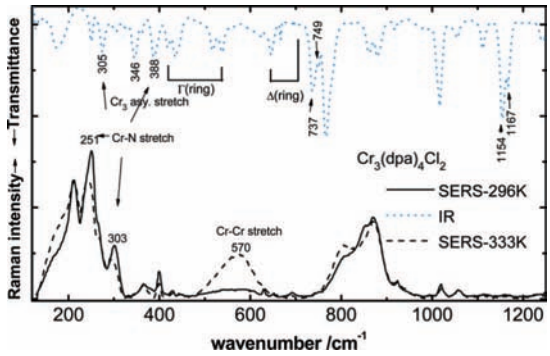

Figure 2. IR spectrum (dotted line) for the solid form and SERS spectra of *u*-$Cr_3(dpa)_4Cl_2$ on silver nanoparticles in aqueous solution at temperatures 296 (solid line) and 333 K (dashed line) (150−1250 cm^{-1}). Symbols are defined in the caption of Figure 1.

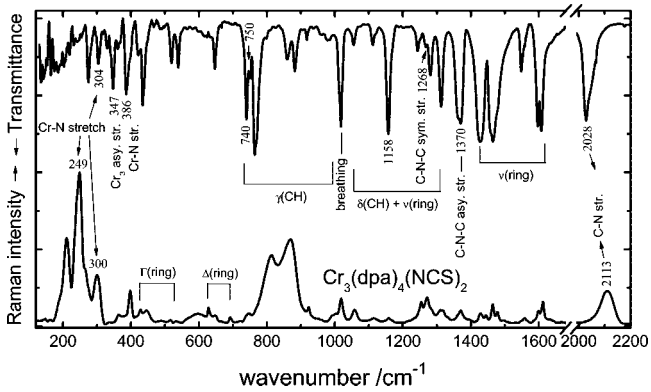

Figure 3. IR spectrum of the solid form and SERS spectra of $Cr_3(dpa)_4(NCS)_2$ on silver nanoparticles in aqueous solution (150−1650 and 2000−2200 cm^{-1}). Symbols are defined in the caption of Figure 1.

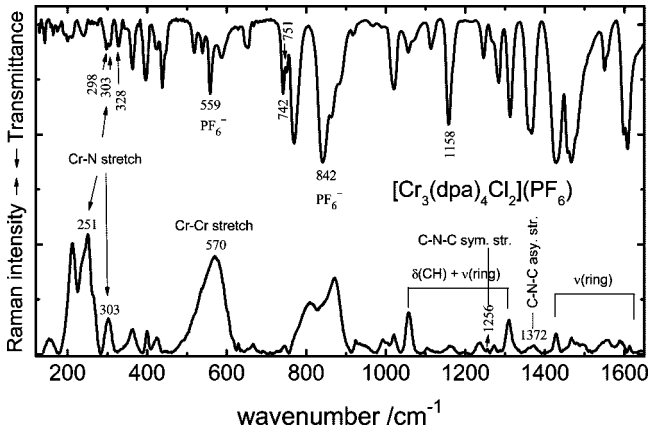

Figure 4. IR spectrum of the solid form and SERS spectra of $[Cr_3(dpa)_4Cl_2](PF_6)$ on silver nanoparticles in aqueous solution (150−1650 cm^{-1}). Symbols are defined in the caption of Figure 1.

bonding to Cr_3^{6+}. Because of deprotonation upon coordination, bands for the N−H out-of-plane bending mode at 595 cm^{-1} and the in-plane bending mode at 1540 cm^{-1} for Hdpa disappear in trichromium complexes. In-plane deformation modes of pyridyl at 668 and 991 cm^{-1} in Hdpa are shifted to 693 and 1019 cm^{-1}, respectively, in $Cr_3(dpa)_4(NCS)_2$.

As reported previously, the IR lines split at 737, 749 cm^{-1} and 1153, 1167 cm^{-1} and the Raman lines at 1010 and 1020 cm^{-1} are found for $Co_3(dpa)_4Cl_2$ in a *u*-form.[28] Similar to the Co_3 complex, the pyridyl lines of *u*-$Cr_3(dpa)_4Cl_2$ are split to 737, 749 cm^{-1} and 1154, 1167 cm^{-1} in IR but there is a single Raman line at 1020 cm^{-1}. The oxidized form $[Cr_3(dpa)_4Cl_2](PF_6)$

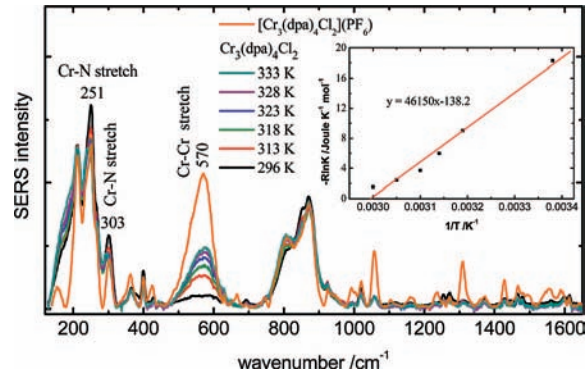

Figure 5. SERS spectra of $Cr_3(dpa)_4Cl_2$ at various temperatures and of $[Cr_3(dpa)_4Cl_2](PF_6)$ at 296 K. Insert: Plot of $-R \ln K$ vs $1/T$.

that has unsymmetric Cr−Cr bond lengths exhibits only a single line at 1158 cm^{-1} in the IR spectrum but split lines at 742 and 751 cm^{-1}. In the SERS spectrum (Figures 4 and 5) the broad line at 570 cm^{-1} indicates the existence of a Cr−Cr quadruple bond. Similarly the SERS spectra of $Cr_3(dpa)_4Cl_2$ display a line at 570 cm^{-1} at increased temperatures, as shown in Figures 3 and 5. According to these experimental results we assign that complex $Cr_3(dpa)_4Cl_2$ exhibits both *s*- and *u*- forms at elevated temperatures and that the *s*-form is the ground state structure. The IR spectrum of $Cr_3(dpa)_4(NCS)_2$ has lines split at 740 and 750 cm^{-1} but a single line at 1158 cm^{-1}; in the Raman spectrum there is a single line at 1019 cm^{-1}, but no line corresponding to the Cr−Cr quadruple bond mode appears at temperatures even up to 60 °C. Accordingly we assign that only an *s*-form exists for this complex.

According to the crystal data, the bond distances within the pyridyl ring for two pyridyls are similar for trichromium complexes in both *s*- and *u*-forms, and even for the oxidized Cr_3 complex. The small splitting in pyridyl vibrational frequencies might hence result from a small variation in bonding to separate Cr atoms. For instance, the bond lengths Co−N(pyridyl) in *u*-$Co_3(dpa)_4Cl_2$ deviate about 0.16 Å, but Cr−N(pyridyl) in $[Cr_3(dpa)_4Cl_2](PF_6)$ deviates only 0.015 Å producing nearly similar pyridyl vibrational wavenumbers for the latter complex. In *u*-$Co_3(dpa)_4Cl_2$ the isolated, high-spin Co^{II} has one electron in the Co−N antibonding molecular ortibal, yielding long metal−nitrogen distance around this atom. With three electrons less than Co, Cr^{II} has no electron to populate this orbital. Hence no large deviation in Cr−N bond distance is expected and consequently less splitting in pyridyl vibrations in Cr_3 complexes.

We assign the broad band at 570 cm^{-1} to the stretching mode of the Cr−Cr quadruple-bond both in the *u*-form of $Cr_3(dpa)_4Cl_2$ and in $[Cr_3(dpa)_4Cl_2](PF_6)$; this vibrational mode is inactive in IR spectra. This wavenumber agrees with the value reported for other metal complexes with a Cr−Cr quadruple bond.[37] The IR lines of $[Cr_3(dpa)_4Cl_2](PF_6)$ at 559 and 841 cm^{-1} are assigned to vibrational modes of PF_6^- by comparison with spectra of $AgPF_6$.

In the region of low frequencies in which metal−metal, metal−ligand, and ligand pyridyl−pyridyl, ring−ring out-of-plane vibrations are located, these modes are the most sensitive to reveal the strength of metal−metal bonding. We assign the IR lines at 429, 365, and 265 cm^{-1} to ligand modes of pyridyl, pyridyl−pyridyl, ring−ring out-of-plane, and C−N−C bending vibrations, respectively, for $Cr_3(dpa)_4(NCS)_2$ because these frequencies are expected to vary least on altering the metal or axial ligand.[27] Compared with those in Hdpa, these modes are blue-shifted. From a comparison with assigned spectra of

$Co_3(dpa)_4Cl_2$ and $Co_3(dpa)_4(NCS)_2$ we assign the SERS lines of $Cr_3(dpa)_4Cl_2$ at 400, 303, 251 cm^{-1}, and IR lines at 388, 305, and 250 cm^{-1} to Cr−N stretching modes.[27] The remaining IR line at 346 cm^{-1} is assigned to the Cr_3 asymmetric stretching of the *s*-form and 275 cm^{-1} to Cr−Cr−Cr bending because they disappear for the oxidized trichromium complex. The line at 275 cm^{-1} is also assigned in part to C−N−C bending. For $Cr_3(dpa)_4(NCS)_2$ the corresponding assignments are SERS lines at 398, 300, 249 cm^{-1}, and IR lines at 386 and 304 cm^{-1} to Cr−N stretching. Lines at 490 cm^{-1} in IR and 489 cm^{-1} in Raman spectra are assigned to axial-ligand NCS bending.

The SERS spectra of $Cr_3(dpa)_4(NCS)_2$ and $Cr_3(dpa)_4Cl_2$ have similarly enhanced intensity in the low wavenumber region and near 800 cm^{-1}. For the formal complex the C−N stretch (in NCS) appears in IR at 2028 cm^{-1} in the solid form but is increased to 2113 cm^{-1} in silver solution; a single line in SERS indicates that both S atoms are bonded to the silver surface under the experimental conditions. The blue-shifted band position of the C−N stretch is due to the less nonbonding electron of the nitrogen atom to antibonding in C−N from bonding to silver. Positions of lines for other modes of both complexes agree within 5 cm^{-1}. The structures are hence similar for these two complexes in an aqueous solution of silver nanoparticles. In SERS the Cr−N lines are more intense than the ligand lines, relative to those in Raman spectra of Co_3 and Ni_3 complexes;[27] moreover no line is assigned to the Cr_3 symmetric stretching mode. These results imply that the metal ion line in the complex lies nearly parallel to the silver surface so that the vibrational motions orthogonal to the metal ion line and silver surface, for example, Cr−N stretching modes, are enhanced according to the surface selection rules whereas motions parallel to the metal ion line, for example, C−N−C stretching and Cr_3 symmetric stretching, are either fairly weak or not observed. Because of poor solubility of this complex in an aqueous solution, a low coverage of the complex on the silver surface is expected. The experimental data imply that, under these conditions, the complex might adsorb on a silver surface with the line of metal ions parallel to the surface and both sulfur or chlorine atoms bonded or adsorbed to silver atoms.

Conversion of *u*- and *s*-Form of $Cr_3(dpa)_4Cl_2$. As shown in Figure 5 relative to $[Cr_3(dpa)_4Cl_2](PF_6)$ that exists in only a *u*-form, the intensity of the line at 570 cm^{-1} for the Cr−Cr quadruple bond of $Cr_3(dpa)_4Cl_2$ is weak at 296 K, indicating a small proportion of the *u*-form. The intensity of this line remains unaltered upon exposure to red light from the laser over 1 h. When the solution is heated to 60 °C, the increased intensity of a line at 570 cm^{-1} indicates conversion of the *s*-form to the *u*-form. For a temperature exceeding 80 °C, the complex decomposed, but the intensity of the line at 570 cm^{-1} showed conversion of the reaction to be nearly complete at 60 °C. We used the spectral intensity of $[Cr_3(dpa)_4Cl_2](PF_6)$ as an external standard to calibrate the intensity of the mode for the Cr−Cr quadruple bond of *u*-$Cr_3(dpa)_4Cl_2$. We first normalized the intensity of lines at low wavenumber and for the region ~800 cm^{-1}, as shown in Figure 5. The intensity of a line of $[Cr_3(dpa)_4Cl_2](PF_6)$ at 570 cm^{-1} is assumed to be that for $Cr_3(dpa)_4Cl_2$ 100% in the *u*-form. The ratio of the measured intensities of the line at 570 cm^{-1} for $Cr_3(dpa)_4Cl_2$ and $[Cr_3(dpa)_4Cl_2](PF_6)$ yielded the proportion of the unsymmetric form. The equilibrium constant K for the reaction *u*-form ↔ *s*-form, equal to the ratio [*u*-form]/[*s*-form] of concentrations, is thus obtained from the variation of spectral intensity with temperature. From the relation $\Delta G = -RT \ln K = \Delta H - T\Delta S$, the reaction enthalpy $\Delta H = 46.2 \pm 3.3$ kJ mol^{-1} and entropy $\Delta S = 138 \pm 10.3$ J K^{-1} mol^{-1} are obtained; the linear plot is shown in the insert of Figure 5.

Rohmer and Bénard[29] calculated the energy of conversion of $Cr_3(dpa)_4Cl_2$ to be 42.3 kJ mol^{-1} for the distorted conformation that has a quadruple bond for Cr−Cr and ferromagnetic coupling between the center Cr and the nonbonded Cr, with respect to the symmetric ground state. These two structures exist with the same spin multiplicity and are thermally accessible according to experimental data, implying formation of bond-stretch isomers. Further theoretical calculations might provide information about the correlation of these two structures on the ground state surface. Exposed to light for 1 h and for temperatures up to 60 °C, complex $Cr_3(dpa)_4(NCS)_2$ remains as a symmetric form, indicating a large barrier for conversion to the *u*-form.

Conclusion

Symmetric and unsymmetric structures of $Cr_3(dpa)_4Cl_2$ are distinguished by means of their IR and SERS spectra. For $Cr_3(dpa)_4(NCS)_2$ only the symmetric form exists under ambient conditions. We obtained the enthalpy and entropy differences between the *s*- and *u*-$Cr_3(dpa)_4Cl_2$ forms to be 46.2 kJ mol^{-1} and 138 J K^{-1} mol^{-1}, respectively. For both trichromium complexes the structure of the ground state is the *s*-form. A line at 570 cm^{-1} is assigned to the Cr−Cr stretching mode of the *u*-form, and a line at 346 cm^{-1} to the Cr_3 asymmetric stretching mode of the *s*-form. According to the spectral intensity and frequency shifts in the SERS spectra, a molecule of Hdpa is likely adsorbed on a silver nanoparticle with the amido nitrogen and pyridyl rings tilted from the silver surface whereas the trimetal complexes with a metal ion line parallel to the silver surface under low coverage condition.

Acknowledgment. National Science Council, Taiwan, provided financial support and the National Center for High-Performance Computing provided computing facilities.

References and Notes

(1) Pyrka, G. J.; El-Mekki, M.; Pinkerton, A. A. *J. Chem. Soc., Chem. Commun.* **1991**, 84.
(2) Wu, L.-P.; Field, P.; Morrissey, T.; Murphy, C.; Nagle, P.; Hathaway, B. J.; Simmons, C.; Thornton, P. *J. Chem. Soc., Dalton Trans.* **1991**, 993.
(3) Hurley, T. J.; Robinson, M. A. *Inorg. Chem.* **1968**, *7*, 33.
(4) Aduldecha, S.; Hathaway, B. J. *J. Chem. Soc., Dalton Trans.* **1991**, 993.
(5) Clérac, R.; Cotton, F. A.; Dunbar, K. R.; Murillo, C. A.; Pascual, I.; Wang, X. *Inorg. Chem.* **1999**, *38*, 2655.
(6) Berry, J. F.; Cotton, F. A.; Daniels, L. M.; Murillo, C. A. *J. Am. Chem. Soc.* **2002**, *124*, 3212.
(7) Berry, J. F.; Cotton, F. A.; Daniels, L. M.; Murillo, C. A.; Wang, X. *Inorg. Chem.* **2003**, *42*, 2418.
(8) Berry, J. F.; Cotton, F. A.; Lu, T.; Murillo, C. A.; Wang, X. *Inorg. Chem.* **2003**, *42*, 3595.
(9) Yang, E.-C.; Cheng, M.-C.; Tsai, M.-S.; Peng, S.-M. *J. Chem. Soc., Chem. Commun.* **1994**, 2377.
(10) Cotton, F. A.; Daniels, L. M.; Jordan, G. T., IV *Chem. Commun.* **1997**, 421.
(11) Cotton, F. A.; Daniels, L. M.; Jordan, G. T., IV; Murillo, C. A. *J. Am. Chem. Soc.* **1997**, *119*, 10377.
(12) Cotton, F. A.; Murillo, C. A.; Wang, X. *J. Chem. Soc., Dalton Trans.* **1999**, 3327.
(13) Cotton, F. A.; Murillo, C. A.; Wang, X. *Inorg. Chem.* **1999**, *38*, 6294.
(14) Clérac, R.; Cotton, F. A.; Daniels, L. M.; Dunbar, K. R.; Kirschbaum, K.; Murillo, C. A.; Pinkerton, A. A.; Schultz, A. J.; Wang, X. *J. Am. Chem. Soc.* **2000**, *122*, 6226.
(15) Clérac, R.; Cotton, F. A.; Dunbar, K. R.; Lu, T.; Murillo, C. A.; Wang, X. *Inorg. Chem.* **2000**, *39*, 3065.
(16) Clérac, R.; Cotton, F. A.; Daniels, L. M.; Murillo, C. A.; Wang, X. *Inorg. Chem.* **2001**, *40*, 1256.
(17) Clérac, R.; Cotton, F. A.; Jeffery, S. P.; Murillo, C. A.; Wang, X. *Inorg. Chem.* **2001**, *40*, 1265.

(18) Clérac, R.; Cotton, F. A.; Jeffery, S. P.; Murillo, C. A.; Wang, X. *J. Chem. Soc., Dalton Trans.* **2001**, 386.

(19) Berry, J. F.; Cotton, F. A.; Lu, T.; Murillo, C. A.; Roberts, B. K. *Inorg. Chem.* **2004**, *43*, 2277.

(20) Clérac, R.; Cotton, F. A.; Daniels, L. M.; Dunbar, K. R.; Lu, T.; Murillo, C. A.; Wang, X. *J. Am. Chem. Soc.* **2000**, *122*, 2272.

(21) Cotton, F. A.; Daniels, L. M.; Murillo, C. A.; Pascual, I. *J. Am. Chem. Soc.* **1997**, *119*, 10233.

(22) Cotton, F. A.; Daniels, L. M.; Murillo, C. A.; Pascual, I. *Inorg. Chem. Commun.* **1998**, *1*, 1.

(23) Clérac, R.; Cotton, F. A.; Daniels, L. M.; Dunbar, K. R.; Murillo, C. A.; Pascual, I. *Inorg. Chem.* **2000**, *39*, 748.

(24) Clérac, R.; Cotton, F. A.; Daniels, L. M.; Dunbar, K. R.; Murillo, C. A.; Pascual, I. *Inorg. Chem.* **2000**, *39*, 752.

(25) Clérac, R.; Cotton, F. A.; Daniels, L. M.; Dunbar, K. R.; Murillo, C. A.; Zhou, H.-C. *Inorg. Chem.* **2000**, *39*, 3414.

(26) Berry, J. F.; Cotton, F. A.; Lu, T.; Murillo, C. A.; Roberts, B. K.; Wang, X. *J. Am. Chem. Soc.* **2004**, *126*, 7082.

(27) Lai, S.-H.; Hsiao, C.-J.; Ling, J.-W.; Wang, W.-Z.; Peng, S.-M.; Chen, I.-C. *Chem. Phys. Lett.* **2008**, *456*, 181.

(28) Benbellat, N.; Rohmer, M.-M.; Bénard, M. *Chem. Commun.* **2001**, 2368.

(29) Rohmer, M.-M.; Bénard, M. *J. Cluster Sci.* **2002**, *13*, 333.

(30) Lin, S.-Y.; Chen, I.-W. P.; Chen, C.-h.; Hsieh, M.-H.; Yeh, C.-Y.; Lin, T.-W.; Chen, Y.-H.; Peng, S.-M. *J. Phys. Chem. B* **2004**, *108*, 959.

(31) S.-M. Peng, unpublished data.

(32) Gibson, C. S.; Colles, W. M. *J. Chem. Soc.* **1931**, 2407.

(33) Frisch, M.; Trucks, G. W.; Schlegel, H. B.; et al. *GAUSSIAN 03*, Revision A.9; Gaussian, Inc.; Pittsburgh, PA, 2003.

(34) Joo, S.-W.; Chung, T. D.; Jang, W. C.; Gong, M.-s.; Geum, N.; Kim, K. *Langmuir* **2002**, *18*, 8813.

(35) Moskovits, M. *J. Chem. Phys.* **1982**, *77*, 4408.

(36) Heaviside, J.; Hendra, P. J.; Paul, S. O.; Freeman, J. J.; Friedman, R. M. *Appl. Spectrosc.* **1981**, *35*, 220.

(37) Cotton, F. A.; Fanwick, P. E.; Niswander, R. H.; Sekutowski, J. C. *J. Am. Chem. Soc.* **1978**, *100*, 4725.

JP8081326